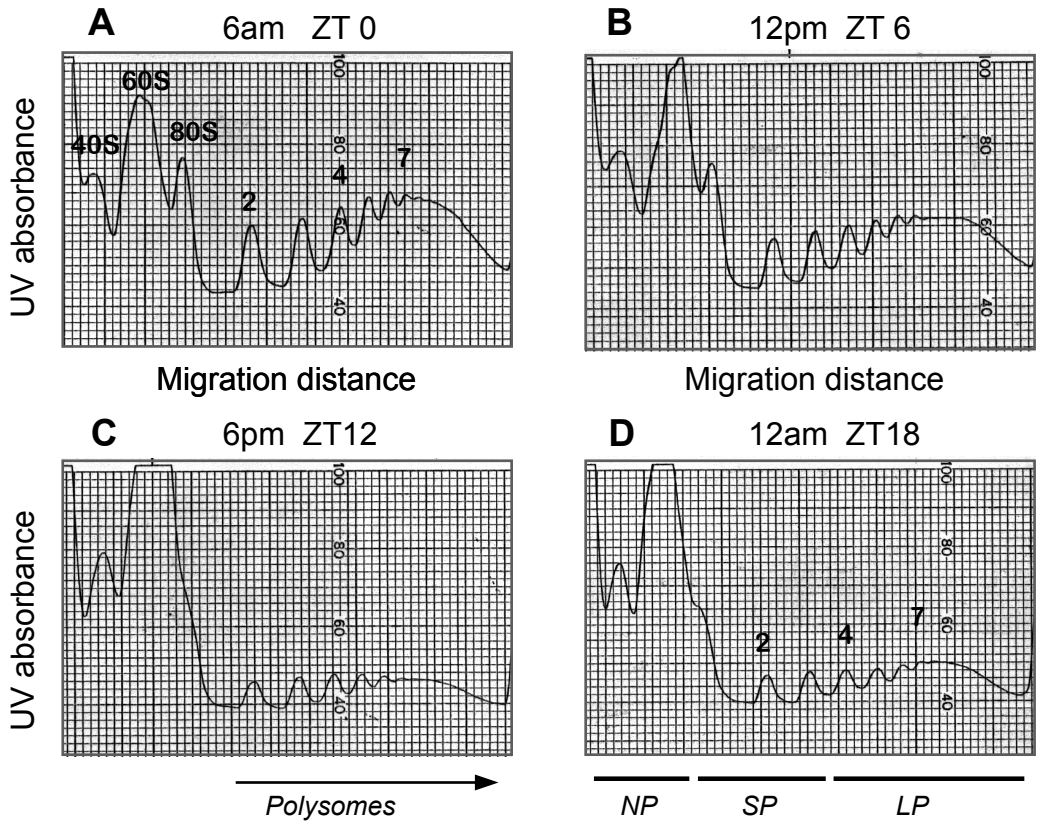

Supplemental Figure 1
Representative polysome gradient UV absorption profiles. Each panel is a scanned trace of pen on graph paper, showing that the fractionation worked as well as reasonably expected. The positions of the 40S, 60S, and 80S ribosome (monosome) are indicated. Peaks with 2, 4, and 7 ribosomes per mRNA are also identified. The regions of the gradient that were pooled into (NP) non-polysomal mRNA, (SP) small polysomes averaging 2 ribosomes per mRNA, and (LP) large polysomes averaging 7 ribosomes per mRNA are indicated in (D). Overall ribosome loading cannot be quantified from these charts because of underlying pigments that contribute to the UV absorption. Ribosome loading for Figure 1 was quantified from UV absorption at 260nm after purifying the RNA from the gradients.

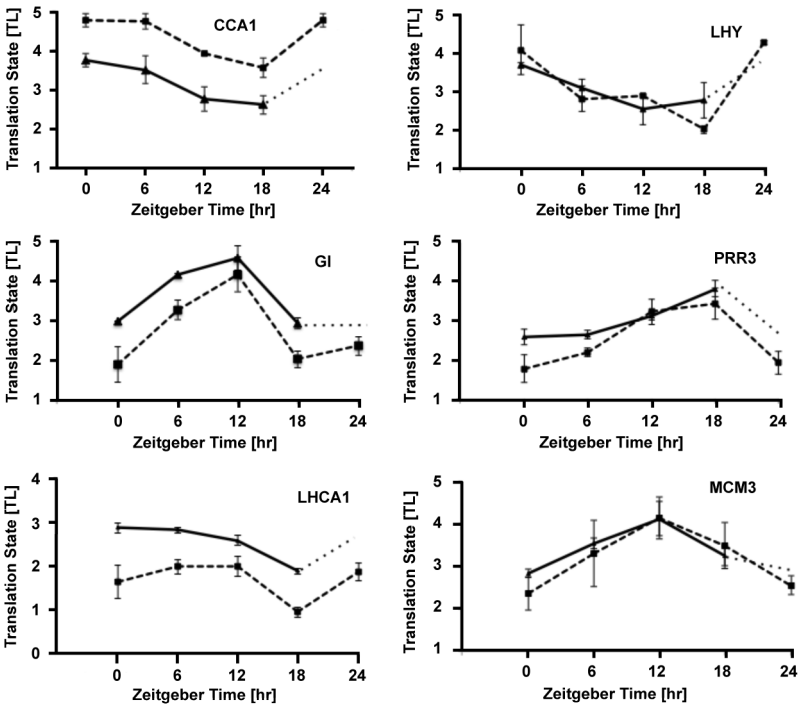

Supplemental Figure 2
Microarray data of mRNA translation state are reproducible by quantitative real-time PCR. The RNA samples from polysome fractionations that were used for the microarray analysis of mRNA translation state were examined independently by qRT-PCR. Solid line: array data. Broken line: qRT-PCR. For qRT-PCR a fifth time point was collected after 24h (ZT24) to confirm that TL values will approach the original TL value at ZT0, thus closing the diurnal cycle. Dotted line: For the array data the ZT0 datapoint was plotted again at ZT24. Error bars show standard deviations from three replications.

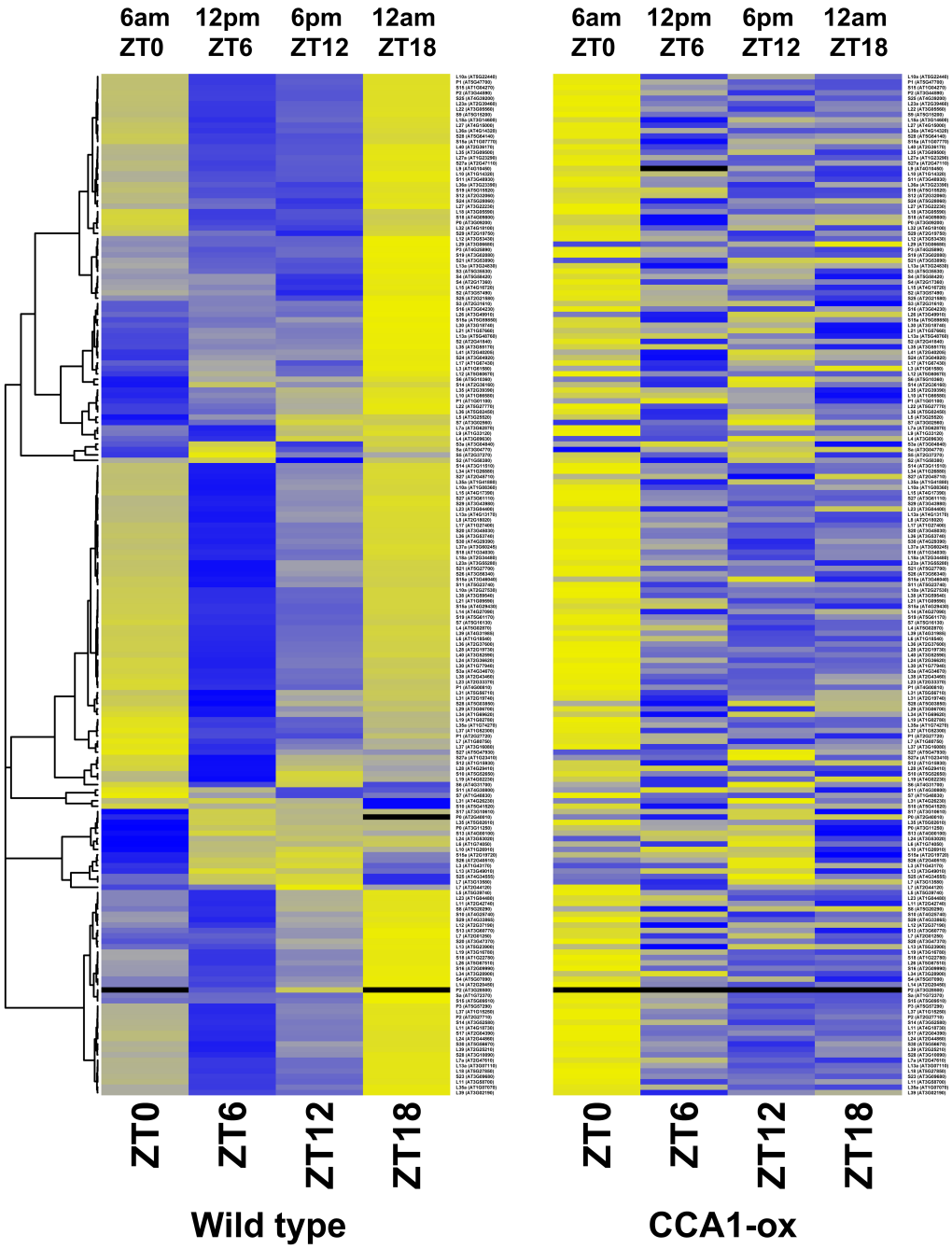

Supplemental Figure 3.
Heatmap of translation states for 189 cytosolic ribosomal protein mRNAs. mRNAs (Barakat et al., 2001; Browning and Bailey-Serres, 2015) were matched to probeset IDs (228 out of the 249 genes). Of these, 189 genes passed a criterion for sufficient and reliable gene expression for at least two time points in wild type. Wild-type ribosome loading data were averaged from three replicates and then clustered hierarchically using their Pearson correlation coefficient, resulting in the dendrogram on the left. The equivalent data for CCA1-ox were not clustered and are displayed in the same gene order as for wild type. For display, the ribosome loading of each gene was z-score transformed, where z=+1 (yellow) indicates a translation state one standard deviation above the mean translation state of the gene. Positive and negative z-scores are yellow and blue respectively. The light period lasts from ZT0 to ZT16. Datapoints with insufficient data, such as low mRNA level, are masked in black. Protein names are readable in the high-resolution version of the figure.

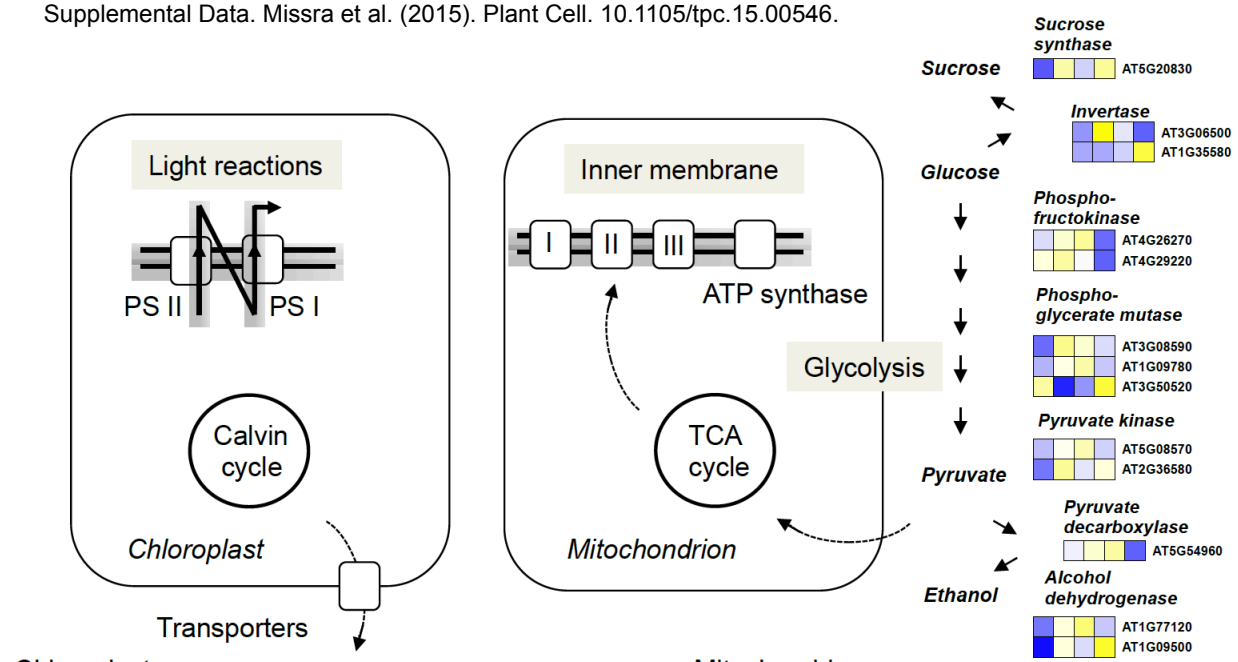

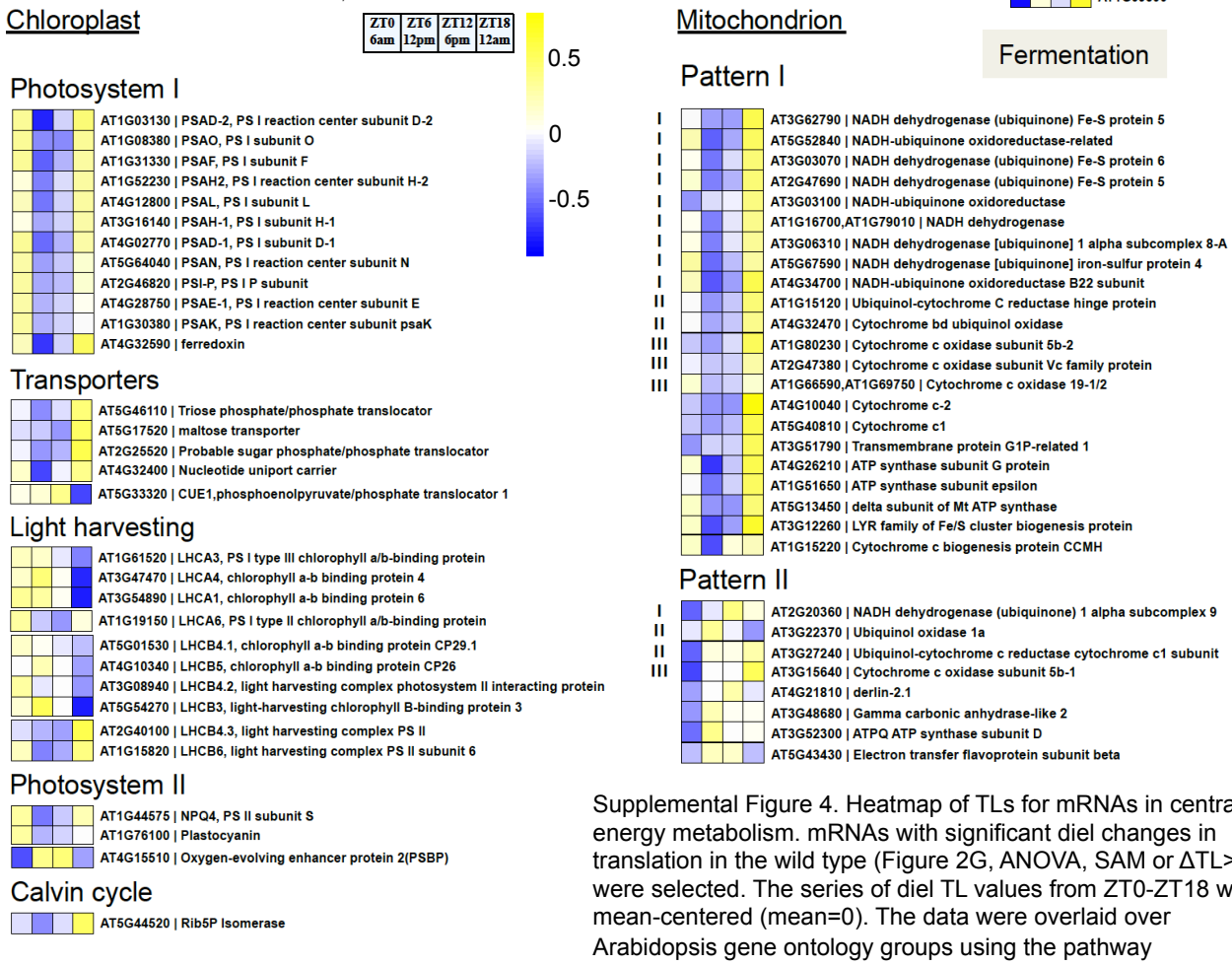

Supplemental Figure 4. Heatmap of TLs for mRNAs in central energy metabolism. mRNAs with significant diel changes in translation in the wild type (Figure 2G, ANOVA, SAM or ΔTL>0.7) were selected. The series of diel TL values from ZT0-ZT18 was mean-centered (mean=0). The data were overlaid over Arabidopsis gene ontology groups using the pathway visualization tool MAPMAN (Thimm et al., 2004). Displayed here are mRNAs involved in energy metabolism in the chloroplast, the mitochondrion, and glycolysis. mRNAs without significant translation cycles are omitted. For example, the ribosome loading of the following glycolytic enzymes was flat: Hexokinase (2 genes), phosphoglucose-isomerase (2 genes), phosphofructokinase (4 other genes), aldolase (7 genes), pyruvate dehydrogenase (3 genes). The tricarboxylic acid cycle also revealed no significant TL cycles. Heatmaps were grouped such that mRNAs with exceptional TL profiles are set apart from the rest.

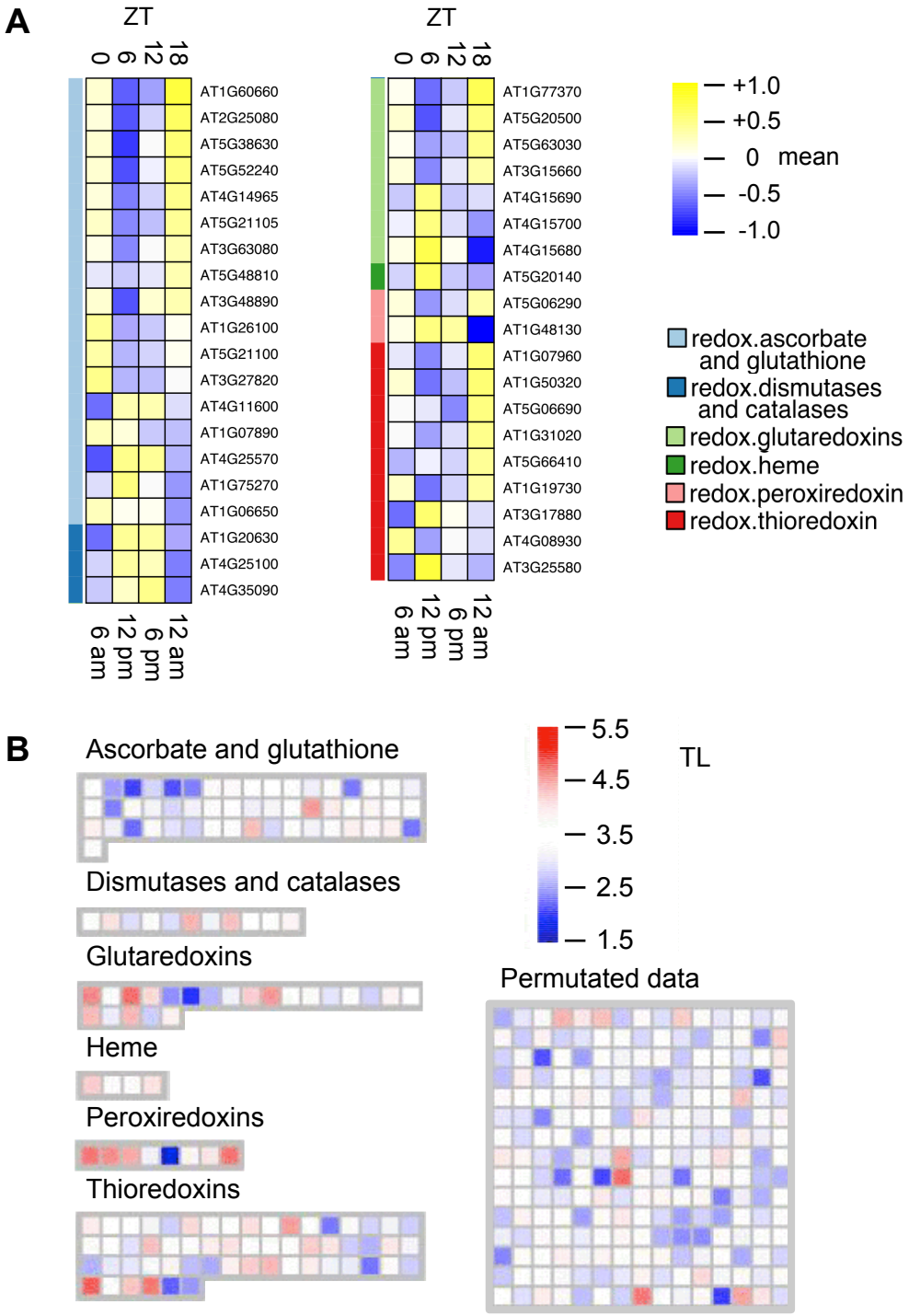

Supplemental Figure 5. Translation states of redox-related mRNAs. (A) Diel cycles of relative translation states. Only mRNAs with significant diel cycles are included in this panel. The TL values were centered on the mean of each time course (mean = 0) for better comparability. Yellow indicates elevated TL and blue is depressed TL. (B) Absolute translation states (TL) of mRNAs were visualized with MAPMAN (Thimm et al., 2004). Each square represents one gene. The data are from the ZT6 (12pm) time point. Except for the ascorbate/glutathione group, the redox mRNAs have relatively high translation states. The panel entitled 'Permutated data' shows a random sampling of translation states from the entire genome.

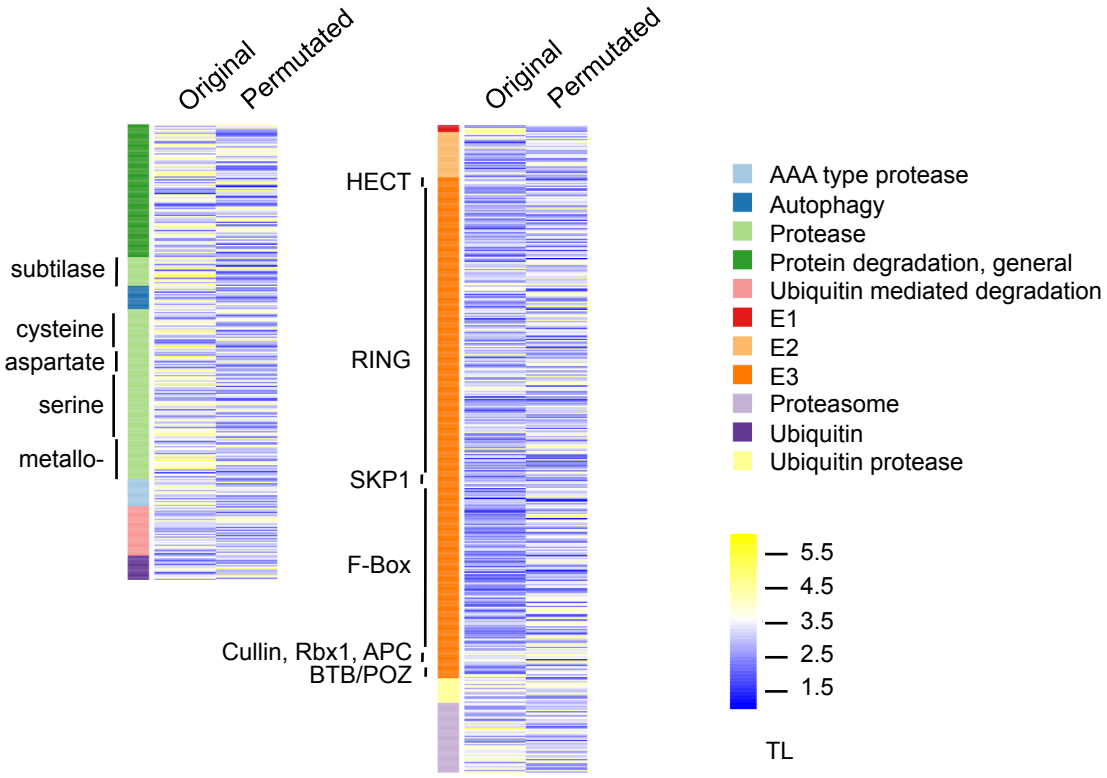

Supplemental Figure 6. Translation states of mRNAs related to protein turnover. The heatmap illustrates the absolute translation states (TL) of mRNAs in various subgroups of the MAPMAN gene ontology term, protein turnover. Each row represents one gene. The actual TL of the gene is plotted in the column labeled ‘original’. The column labeled ‘permutated’ shows the distribution of TL values after randomization. The data are from the ZT6 (12pm) time point. Proteases and including 26S proteasome subunits tend to have notably higher translation states than mRNAs for E3 ubiquitin ligases.

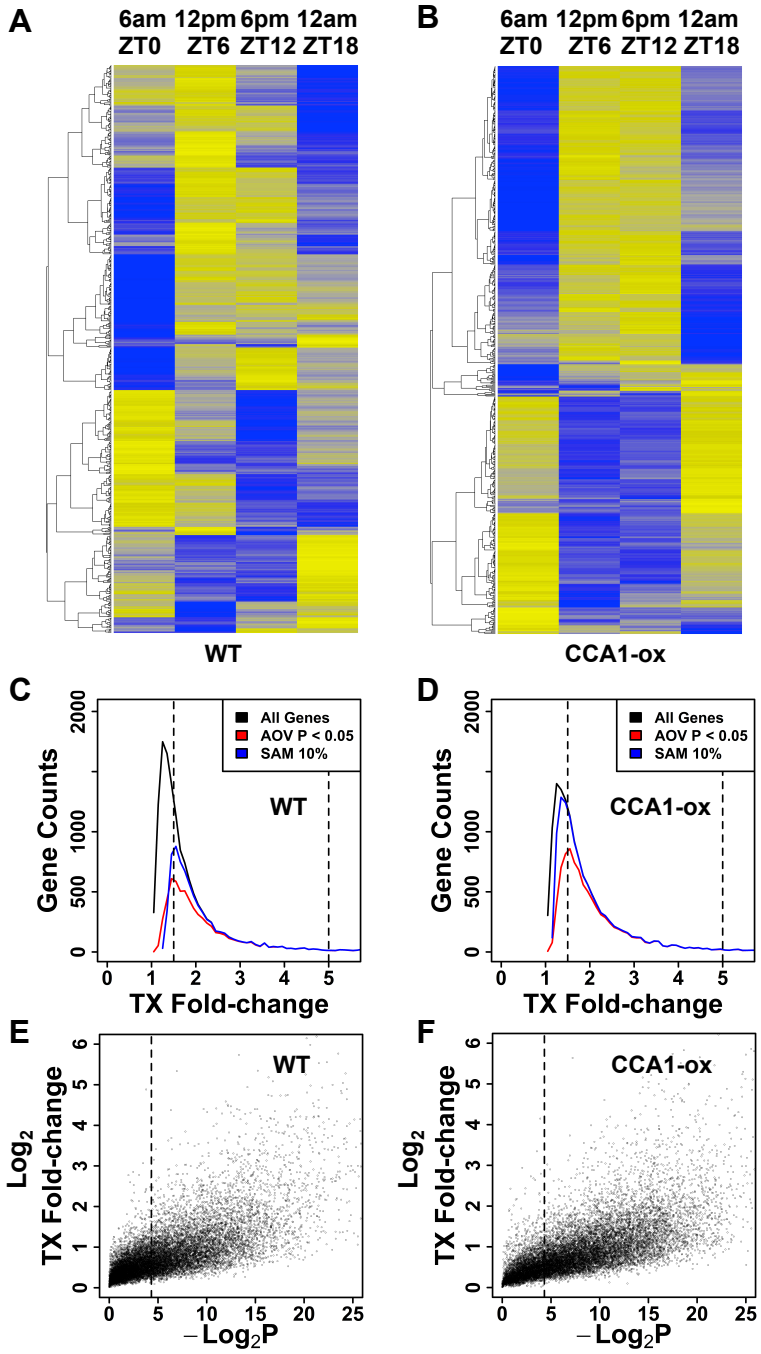

Supplemental Figure 7.
Diel transcript levels in wild type and CCA1-ox. Heat map of total mRNA levels obtained under long day conditions at 6am (ZT0), 12pm (ZT6), 6pm (ZT12), and 12am (ZT18). Data are averages from three biological replicates. Only mRNAs with a fold-change higher than 5-fold are included. (A) WT, 615 genes, (B) CCA1-ox. Transcript levels are displayed after z-score transformation (yellow=high). The clustering tree on the left reveals how, in CCA1-ox, most mRNAs fall into two large clusters that correlate with light (12pm and 6pm) and darkness (6am and 12am). In contrast, in wild type, transcript levels fall into four major clusters that were less prone to reflect the light environment. Panels (C) and (D) show a line histogram of transcript fold changes for the entire dataset (13,625 genes) similar to Figure 2C and D. Panels (E) and (F) show the relation between ANOVA p-value (AOV) and fold-change in transcript level for 14,218 genes (volcano plots). The stippled line represents p=0.05.

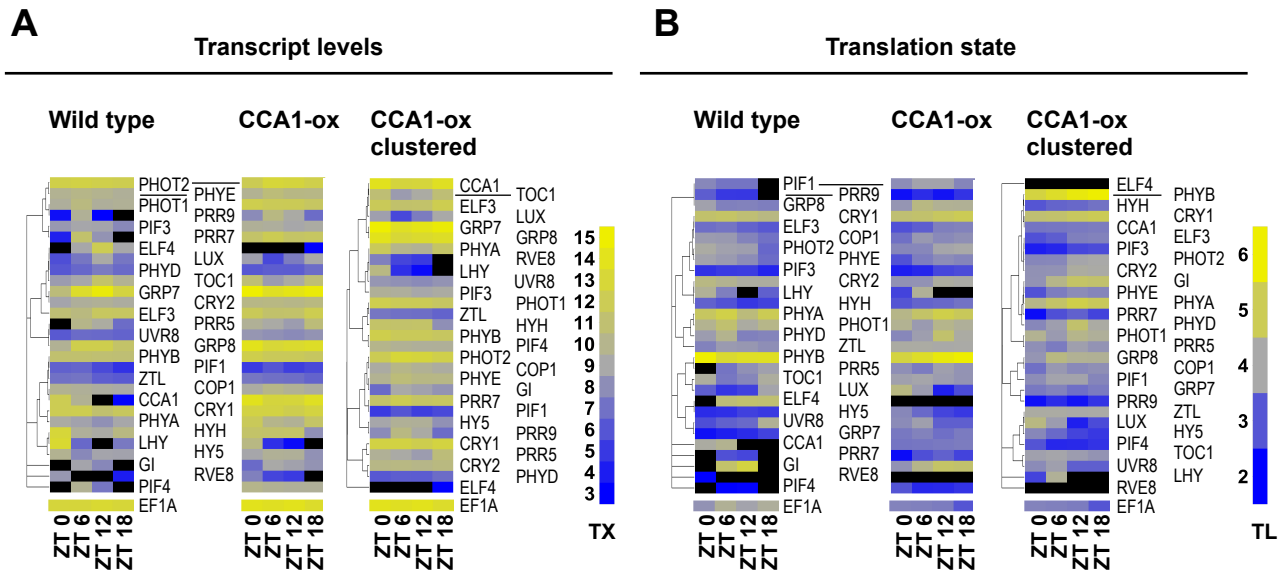

Supplemental Figure 8. Diel cycles of translation states and mRNA transcript levels for clock-associated genes.

(A) Transcript abundance, averaged over three replicates. Abundance values are log2-transformed expression signals (yellow=high). Black indicates that the gene did not pass our pre-filter for that time point. Previously described clock-regulated genes were hand-selected, focusing on the central oscillator, the light input pathways, and selected outputs. EF1A was included for comparison as a weakly cycling mRNA. (Left) WT. Genes were clustered using hierarchical clustering based on Pearson coefficients, with replicates averaged. (Middle) Data from CCA1-ox were displayed as for WT, and the genes are ordered according to the WT clustering tree. Gene names are printed between left and middle panels and apply to both panels. (Right) CCA1-ox data were re-clustered on their own; gene names are printed on the right.

(B) Translation patterns of clock-associated genes are displayed as in panel A. Translation states (TL) were calculated as described in Methods, where TL = 3 corresponds to an estimated average of three ribosomes per mRNA.

Supplemental Data. Missra et al. (2015). Plant Cell. 10.1105/tpc.15.00546

Transcript peak – CCA1-ox

6 am ZT 0

Cellular Component	Annotated	Present	Enrichment	FDR	WT
Nucleus	4967	1589	1.1	1E-14	1.1
├ Mediator complex	23	10	1.6		1.3
├ Spliceosome complex	11	7	2.3		2.1
└ Nucleolus	244	123	1.8	4E-12	1.5
Ribonucleoprotein	403	179	1.6	5E-11	1.2
└ Cytosolic ribosome	228	108	1.7	5E-09	1.3
Cullin-Ring E3 ligase	122	51	1.5	5E-03	1.4
Biological Process					
RNA-biology					
├ Translation	459	186	1.5	5E-08	1.1
├ RNA methylation	171	115	2.4	3E-24	**1.1**
├ rRNA processing	253	62	0.9		1.1
│ └ Cleavage	18	14	2.8	3E-04	2.2
├ RNA splicing	88	52	2.1	3E-08	1.9
├ mRNA catabolism	102	48	1.7	5E-04	1.5
└ mRNA transport	60	39	2.3	7E-08	2.7
Protein local. to organelle	491	238	1.7	1E-22	1.8
├ Mitochondrion	98	60	2.2	3E-10	2.3
├ Nucleocytoplasm	177	100	2.0	1E-15	1.6
├ Peroxisome	95	59	2.2	2E-10	2.2
└ Vesicle mediated	484	229	1.7	3E-18	**1.0**
Photoperiodism	148	94	2.3	2E-17	3.3
├ Long-day	19	11	2.1		2.4
└ Reg. circadian rhythm	37	22	2.1	1E-05	**1.4**
Glucosinolate biosynthesis	161	11	0.2		0.3
Phosphatidylinositol bios.	99	50	1.8	3E-05	**0.8**
Fatty acid catabolism	188	92	1.8	2E-08	1.5
Cell division	446	101	0.8		0.7
└ Cytokinesis	201	26	0.5		**0.3**

12 pm ZT 6

Cellular Component	Annotated	Present	Enrichment	FDR	WT
Chloroplast	2774	865	1.5	1E-42	**1.0**
├ Stroma	606	220	1.7	1E-18	**1.0**
│ ├ Nucleoid	27	18	3.1	7E-06	**1.0**
│ └ Plastoglobule	58	24	2.0	5E-03	2.5
├ Plastid envelope	534	195	1.7	4E-15	1.2
├ Thylakoid	378	141	1.8	9E-12	1.6
│ └ Membrane	281	106	1.8	3E-09	1.7
│ └ Photosystem	63	23	1.7	4E-02	2.2
│ ├ PS II	42	12	1.3		2.0
│ │ └ React. center	12	1	0		0
│ └ PS I	21	11	2.5	2E-02	2.6
│ └ React. center	11	6	2.6	1E-02	3.0
└ Lumen	68	20	1.4		1.8
Chromosome	144	52	1.7	3E-04	1.5
└ Nucleosome	43	22	2.4	2E-04	**1.4**
Biological process					
Photosynthesis	400	150	1.8	2E-12	1.4
└ Light reaction	309	122	1.9	8E-12	1.5
└ PS II light harvesting	27	18	3.2	2E-05	**1.0**
NADP metabolism	198	66	1.6	8E-04	1.4
Glyceraldehyde-3-P metab.	227	95	2.0	6E-11	**1.3**
Disaccharide metabolism	188	87	2.2	9E-13	1.5
Oligosaccharide metab.	208	89	2.0	7E-11	1.5
Starch metabolism	216	100	2.2	1E-16	1.6
Pentose-P shunt	195	66	1.6	5E-04	1.4
Plastid transcription	73	37	2.4	9E-07	**1.0**
Amino acid biosynthesis	512	143	1.3	2E-03	1.1
Pigment metabolism	305	148	2.3	1E-26	1.6
├ Chlorophyll	184	85	2.2	2E-12	2.1
├ Isoprenoid biosynth.	381	153	1.9	1E-15	1.3
├ Carotenoids	105	64	2.9	2E-16	**1.3**
└ Flavonoids	185	66	1.7	1E-04	1.5
Glucosinolate biosynthesis	161	43	1.3		1.8
rRNA processing	253	83	1.6	2E-04	**0.9**
Response to red light	86	36	2.0	3E-04	1.7
Inositol phosphate biosynth.	61	45	3.5	4E-16	**2.1**
Cell division	446	103	1.1		1.4
└ Cytokinesis	201	52	1.2		2.2

Transcript peak – CCA1-ox

6 pm ZT 12

Cellular Component	Annotated	Present	Enrichment	FDR	WT
Chloroplast	2774	701	1.5	2E-35	1.5
├ Stroma	588	222	2.2	2E-33	1.8
│ ├ Clp protease	8	3	2.2		**1.0**
│ └ Plastoglobule	58	20	2.0	7E-03	**0.3**
├ Plastid envelope	534	180	2.0	1E-20	1.5
└ Thylakoid	378	140	2.2	4E-20	**1.2**
├ Membrane	283	107	2.2	3E-16	**1.1**
│ └ O_2 evolving cx.	19	9	2.8	2E-02	**1.2**
└ Lumen	68	33	2.9	2E-08	**1.3**
Mitochondrial part	229	47	1.2		1.1
Cytosolic ribosome	228	67	1.7	2E-05	**1.0**
Vacuole	654	139	1.3	1E-02	1.3
Apoplast	247	89	2.1	4E-12	1.6
Chromosome	144	26	1.1		1.9
└ Nucleosome	43	3	0.4		2.6
Biological Process					
PS, light reaction	309	107	2.0	4E-12	**1.0**
└ PS II assembly	170	62	2.1	4E-08	**0.9**
NADP metabolism	198	94	1.7	2E-20	1.5
Glucose catabolism	455	165	2.1	2E-20	**1.4**
Pentose-P shunt	195	94	2.8	2E-20	**1.5**
Polysaccharide synthesis	428	113	1.5	2E-05	1.8
└ Starch	182	80	2.5	2E-15	3.2
Amino acid biosynthesis	512	148	1.7	9E-10	1.5
├ Cysteine	207	79	2.2	2E-11	**1.2**
└ Peptidyl-Cys-S-nitrosylation	15	12	4.6	4E-06	**1.0**
Chlorophyll biosynthesis	121	46	2.2	1E-08	**0.9**
Glucosinolate biosynthesis	161	79	2.8	2E-18	2.3
rRNA processing	253	77	1.8	4E-06	**1.1**
Response to metal ion	471	140	1.7	4E-10	1.5
DNA replication	190	61	1.9	8E-06	2.4
Pyrimidine nucleotide bios.	139	23	1.0		3.0
Cell division	446	89	1.2		0.9
└ Cytokinesis	201	62	1.8	3E-05	1.3

12 am ZT 18

Cellular Component	Annotated	Present	Enrichment	FDR	WT
Nucleus	4967	1198	1.2	2E-10	0.9
Plasma membrane	2110	539	1.2	1E-06	1.6
Cell wall	174	50	1.4		2.2
Golgi apparatus	673	152	1.1		1.5
Biological Process					
Cellulose metabolism	130	34	1.3		2.1
Pectin metabolism	47	14	1.4		3.6
Cell wall organization	353	80	1.1		1.8
Cell wall loosening	18	2	0.5		4.4
(An)ion transport	385	117	1.5	2E-04	2.1
└ Inorganic	179	72	1.9	3E-07	2.7
├ Nitrate	122	49	1.9	3E-05	2.6
├ Ammonium	25	13	2.5	1E-02	3.9
└ Transition metal	104	34	1.6		1.2
Amino acid import	60	26	2.1	2E-03	2.8
Amine metabolism	182	43	1.1		1.7
Glucosinolate biosynthesis	161	15	0.5		0.9
Reg. of defense response	434	144	1.6	1E-07	2.0
├ Response to chitin	277	104	1.8	2E-08	2.1
├ -"- to salicylic acid	337	102	1.5	6E-04	1.7
├ Cell death	395	132	1.6	3E-07	2.0
└ Respiratory burst	80	34	2.1	3E-04	2.9
Response to darkness	29	13	2.2		2.4
Response to hypoxia	40	16	1.9		1.8
-"- to unfolded protein	139	58	2.0	1E-06	2.1
Cell division	446	89	1.0		**0.4**
└ Cytokinesis	201	36	0.9		**0.2**

Supplemental Figure 9.

Gene ontology analysis of diurnal transcript levels in the CCA1-ox strain. Diurnal transcript levels were filtered for a difference between peak and trough using SAM with a 10% FDR without a fold-change cutoff. Groups of mRNAs with peaks at the given times were examined for enrichment of functional annotation categories using TOPGO. mRNAs lacking a peak were also tested for GO enrichment but did not return significant biases. The total number of genes in this dataset that falls under a given GO term is given as 'Annotated', the number that has a transcript peak at the given time is given as 'Present', along with the fold-overrepresentation (Enrichment) of this class in the CCA1-ox. FDR indicates the likelihood of false discovery. For comparison, the enrichment factor for each term in WT is also shown. If the enrichment factor in CCA1-ox is more than 1.5 fold higher than in wild type, the WT enrichment value is printed bold red; if the wild-type enrichment is 1.5 fold higher, then the WT enrichment value is underlined and green.

Translation peak – CCA1-ox

6 am ZT 0

Cellular Component	Annotated	Present	Enrichment	FDR
Chloroplast	2494	516	1.1	4E-02
└ Thylakoid	407	127	1.6	2E-08
├ Membrane	271	97	1.9	9E-10
├ Photosystem	42	27	3.4	3E-09
├ PS II	27	13	2.5	4E-03
└ React. center	plastid encoded			
└ PS I	15	14	4.9	1E-08
└ React. center	8	8	5.3	2E-05
└ b6f complex	plastid encoded			
└ Lumen	65	19	1.5	
Ribonucleoprotein	375	157	2.2	3E-23
├ Ribosome	307	139	2.4	4E-24
├ Cytosolic ribosome	223	110	2.6	5E-23
├ Large subunit	90	57	3.3	1E-18
└ Small subunit	72	32	2.3	7E-06
└ Plastid ribosome	5	0	0	
└ snRNP	26	10	2.0	8E-02
Nucleolus	237	60	1.3	5E-02
Prefoldin complex	9	7	4.1	2E-03
Mitochondrion	1349	274	1.1	
├ Mito. inner membrane	151	44	1.5	1E-02
└ Respiratory chain	69	28	2.1	2E-04
├ Complex I NDH	43	20	2.5	3E-04
├ Complex II	8	4	2.6	
└ Complex III	14	3	1.1	
└ Mito. envelope	186	51	1.4	2E-02
Vacuole	600	174	1.5	1E-08
Endoplasmic reticulum	381	101	1.4	1E-03
H+ ATPase, V-type	11	9	4.3	1E-04
Biological Process				
Translation	426	152	1.9	7E-13
Carbohydrate catabolism	516	147	1.5	1E-05
├ Glucose	451	141	1.6	7E-08
└ Pentose-P shunt	195	60	1.6	3E-02
Phospholipid biosynthesis	354	103	1.5	3E-04
Photorespiration	149	52	1.8	4E-02
Phosphatidylinositol bios.	90	46	2.7	5E-09
RNA methylation	165	64	2.0	6E-07
Divalent metal ion transport	175	61	1.8	7E-05
Cysteine biosynthesis	202	64	1.6	1E-03
Vesicle mediated transport	461	125	1.4	1E-03
α-amino acid biosynthesis	386	95	1.3	9E-02

12 pm ZT 6

Cellular Component	Annotated	Present	Enrichment	FDR
Chloroplast	2494	349	1.8	4E-30
├ Stroma	558	118	2.7	4E-22
└ Nucleoid	31	11	4.5	2E-04
├ Plastid envelope	495	89	2.3	3E-12
└ Thylakoid	407	70	2.2	1E-08
├ Membrane	271	35	1.6	3E-02
└ Photosystem	42	3	not enriched	
└ Lumen	77	15	2.4	1E-02
Signal recognition particle	9	6	8.3	3E-04
Nuclear chromatin	15	4	3.4	
Proteasome complex	44	10	2.9	2E-02
Biological process				
Carboxylic acid metab.	1425	185	1.6	1E-09
Ribonucleotide metabolism	249	39	1.9	1E-03
Amino acid metabolism	694	107	1.9	4E-09
└ α-amino acid biosynth.	386	52	1.7	3E-03
├ Aromatic	86	23	3.3	1E-05
├ Arginine	9	3	4.1	
├ Serine family	208	29	1.7	3E-02
├ Valine, (Iso)leucine	14	5	4.4	4E-02
├ Aspartate family	111	13	1.5	
├ Thr metabolism	14	7	6.2	1E-03
├ Glutamine family	20	3	1.9	
├ Lysine	7	1	1.8	
├ Proline	5	1	2.5	
└ Histidine	8	1	1.6	
rRNA processing	247	48	2.4	7E-07
tRNA metabolic process	108	34	3.9	8E-10
└ tRNA aminoacylation	39	12	3.8	8E-04
S-compound metabolism	499	72	1.8	3E-05
├ Fe-S cluster assembly	95	23	3.0	4E-05
├ Glucosinolate metab.	173	32	2.3	2E-04
└ Cysteine biosynthesis	202	27	1.7	6E-02
Protein targeting to plastid	61	12	2.4	4E-02
Photosystem II assembly	146	28	2.4	3E-04
Isoprenoid biosynthesis	351	62	2.2	3E-07
└ Carotenoids	103	25	3.0	2E-05

Translation peak – CCA1-ox

6 pm ZT 12

Cellular Component	Annotated	Present	Enrichment	FDR
Chloroplast	2494	298	1.2	3E-03
├ Stroma	558	73	1.4	
└ Ribosome	5	0		
└ Thylakoid	407	not enriched		
Chromosome	125	21	1.7	
└ Chromatin	65	12	1.9	
Molecular Function				
Metalloendopeptidase	38	17	4.6	4E-06
ATP binding	1089	157	1.5	1E-05
Biological Process				
Plastid organization	375	74	2.0	3E-06
└ Localization	103	23	2.3	5E-03
Photosynthesis	318	39	not enriched	
Carbohydrate biosynthesis	676	89	1.3	3E-02
└ Polysaccharide	455	68	1.5	8E-03
└ Starch	179	30	1.7	3E-02
Cell cycle	552	82	1.5	3E-03
└ Cell division	393	63	1.6	3E-03
└ Cytokinesis	178	42	2.4	1E-05
Microtubule process	241	51	2.2	2E-05
Carotenoid biosynthesis	103	21	2.1	2E-02
tRNA aminoacylation	39	9	2.4	
Histone lysine methylation	178	34	2.0	5E-03
├ H3-K9	136	29	2.2	2E-03
└ H3-K4	8	3	3.8	

12 am ZT 18

Cellular Component	Annotated	Present	Enrichment	FDR
Nucleus	4451	402	1.2	3E-04
Molecular Function				
ATP binding	1089	140	1.8	5E-10
├ Protein kinase	577	82	2.0	7E-08
└ Helicase	99	16	2.2	4E-02
Biological Process				
mRNA catabolism	98	20	2.7	6E-03
Gene silencing by RNA	236	33	1.9	4E-02
Chromatin silencing	185	26	1.9	6E-02
Protein phosphorylation	668	86	1.7	2E-04
Protein glycosylation	193	31	2.1	6E-03
N compound catabolism	315	32	1.4	
Actin nucleation	75	14	2.5	6E-02
Cell cycle	552	63	1.5	4E-02
Gravitropism	129	35	3.6	2E-08

Supplemental Figure 10. Gene ontology analysis of diurnal changes in translation state in CCA1-ox. Translation states of nuclear-encoded genes were classified according to the time of peak TL. Genes were filtered for a significant TL cycle by selecting with SAM (Tusher, 2001) at an FDR of <0.1, or ANOVA with p<0.05 or Delta TL>0.7. Genes with TL peaks were distributed as follows: peak at 6am: 2140 genes; 12pm: 899; 6pm:1112; 12am: 842. GO analysis was performed with TOPGO, using all 10,942 reliably expressed genes as a background set. FDR values below 1E-10 are colored dark green, those between 1E-10 and 1E-05 are colored medium green, and those between 1E-05 and 5E-02 are light green. Abbreviations: PS, photosystem; NDH, NADH dehydrogenase; P, phosphate; snRNP, small nucleolar ribonucleoprotein particle, H3-K, histone 3-lysine.

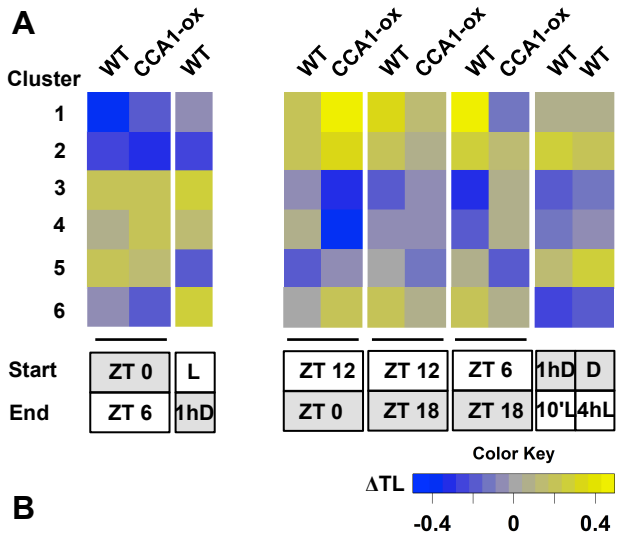

B

	p-value		p-value
Cluster 1 (1335 genes)			
CC: Vacuole, ER	2E-5	BP: RNA methylation	3E-3
CC: Ribosome	3E-4	BP: Proteasome assembly	2E-2
CC: Mitochondrion	5E-4	BP: S-compound metabolism	2E-2
Cluster 2 (2525 genes)			
MF: Ribosome	4E-5	BP: Photoperiodism	8E-5
		BP: Phosphatidyl-inositol	2E-6
Cluster 3 (2499 genes)			
MF: ATP-binding	6E-29	BP: Meristem development	1E-7
		BP: Cytoskeleton	1E-6
Cluster 4 (772 genes)			
MF: Cellulose synthase	2E-3	BP: Polysacch. biosynthesis	7E-4
		BP: mRNA metabolism	7E-4
Cluster 5 (1304 genes)			
CC: Chloroplast	4E-6	BP: RNA splicing	2E-2
Cluster 6 (743 genes)			
CC: Golgi	3E-8	BP: Root hair development	5E-6
CC: Cell wall	7E-8	BP: Glucose catabolism	2E-5
CC: Vacuole	4E-6	BP: Cysteine biosynthesis	6E-5

Supplemental Figure 11. The diel translation responses to light-dark changes are only partially correlated with responses to short-term light-dark shifts. Data from wild type and CCA1-ox were co-clustered together with mRNAs known to be regulated by a 1 hour exposure to darkness (L-> 1hD), followed by reillumination for 10 minutes (1hD->10'L; Juntawong et al., 2012), as well as with mRNAs known to be translationally regulated when dark-grown, etiolated, seedlings are exposed to four hours of light (D->4hL; Liu et al., 2012). Public microarray data sets GSE34231 and GSE29657 were obtained from the Gene Expression Omnibus (GEO) repository at http://www.ncbi.nlm.nih.gov/geo/. Raw data were processed as described above, and probes with marginal ("M") or present ("P") expression signals in all polysome and total RNA fractions within each data set were retained, resulting in 9,178 probes of sufficient quality in common among the two public data sets and our own. TL was calculated for each probe in the public data as TL = polysomal/total RNA, and TL in our data was calculated as described earlier. ΔTL values were calculated for eleven comparisons between experimental conditions as the difference in mean TL. Hierarchical clustering of the genes on the basis of their ΔTL across the eleven comparisons was performed, using the Pearson coefficient as the similarity metric. The resulting cluster tree was cut into six clusters, and within each cluster, the ΔTL values were averaged over all genes. (A) displays the eleven mean ΔTL values for each cluster (yellow=translational stimulation). Treatments are indicated at the bottom where gray shading stands for dark condition (e.g. ZT18) and no shading stands for light condition (e.g. ZT6). (B) GO enrichment analysis was performed on the genes in each cluster using *topGo*. Key enriched terms are shown along with the false discovery corrected p-value. BP, biological process, MF, molecular function, CC, cellular compartment.

Supplemental Data. Missra et al. (2015). Plant Cell. 10.1105/tpc.15.00546.

Supplemental Table 1. Oligonucleotides

Oligonucleotide	AGI Number	Sequence 5' to 3'
RPL26B F	AT5G67510	GTTCTCATGAGCTCGCCGTT
RPL26B R	AT5G67510	GAACGTCCCACGAACAACTT
LHCA1 F	AT3G54890	CAGCTTACCTTGACGGTTCTG
LHCA1 R	AT3G54890	GAGCTCTGACTCTTTGTATCTCTCAA
GIGANTEA F	AT1G22770	GCAACAATACGGTGCCTTTC
GIGANTEA R	AT1G22770	TGGGTATGGAGCTTTGGTTC
EF1A F	AT5G60390	TCTCCGAGTACCCACCTTTG
EF1A R	AT5G60390	CTCCAGTTGGGTCCTTCTTG
CCA1 F	AT2G46830	CGGGTGTGAATGATGGAAAAGA
CCA1 R	AT2G46830	CGATCTTCATTGGCCATCTCAG
CAB4 F	AT3G47470	AGAGCTAGCAAACGGGAGGT
CAB4 R	AT3G47470	TCAGACAAGTGCTGCAACAGA
LHY F	AT1G01060	GACAACGCGGTTCAAGATG
LHY R	AT1G01060	TGCCAAGGGTAGTTTTGCAT
MCM3 F	AT5G46280	CAACAACAATGGGGTTGGAG
MCM3 R	AT5G46280	GCCATCGCTGATCATCACTT
PRR3 F	AT5G60100	TGACAAGAAGTCGGTGAAACC
PRR3 R	AT5G60100	CCACCACTACTCCCACTTTCA

Supplemental Table 2. Arabidopsis Genome Identifiers (AGI) of selected genes.

Gene	AGI Number
CAB4	AT3G47470
CCA1	AT2G46830
COP1	AT2G32950
CRY1	AT4G08920
CRY2	AT1G04400
EF1A	AT5G60390
ELF3	AT2G25930
ELF4	AT2G40080
GI	AT1G22770
GRP7/CCR2	AT1G06820
GRP8/CCR1	AT4G39260
HY5	AT5G11260
HYH	AT3G17609
LHCA1	AT3G54890
LHCB3	AT5G54270
LHY	AT1G01060
LTP1	AT2G38540
LUX	AT3G46640
MCM3	AT5G46280
MRPL11	AT4G35490
PEPC1	AT1G17710
PHYA	AT1G09570
PHYB	AT2G18790
PHYC	AT5G35840
PHYD	AT4G16250
PHYE	AT4G18130
PHOT1	AT3G45780
PHOT2	AT5G58140
PIF1	AT2G20180
PIF3	AT1G09530
PIF4	AT2G43010
PGR5	AT2G05620
PRR3	AT5G60100
PRR5	AT5G24470
PRR7	AT5G02810
PRR9	AT2G46670
RCE1	AT4G36800
RPL26B	AT5G67510
RVE8	AT3G09600
SRR1	AT5G59560
TOC1	AT5G61380
UVR8	AT5G63860
ZTL	AT5G57360

Supplemental References

Thimm, O., Blaesing, O., Gibon, Y., Nagel, A., Meyer, S., Krüger, P., Selbig, J., Müller, L.A., Rhee, S.Y. and Stitt, M. (2004). MAPMAN: a user-driven tool to display genomics data sets onto diagrams of metabolic pathways and other biological processes. Plant J **37:** 914-39.

Browning, K.S. and Bailey-Serres, J. (2015). Mechanism of cytoplasmic mRNA translation. The Arabidopsis Book **13**:e0176.